

## Experimental study of the growth period of wall-attached bubbles

Lu Lin, Ran Li, Jingjie Feng\*, Xiaolong Cheng, Youquan Yuan and Zhenhua Wang

State Key Laboratory of Hydraulics and Mountain River Engineering, Sichuan Univ., 24 South Section 1, Ring Rd. No. 1, Chengdu, Sichuan 610065, China

\*Corresponding author. E-mail: fengjingjie@scu.edu.cn

### ABSTRACT

Due to dam discharge, waterfalls, sudden increases in water temperature and oxygen production by photosynthesis, the total dissolved gas (TDG) in water is often supersaturated, which may have serious effects on aquatic ecology. Wall-attached bubbles formed during the TDG release process and the generation and departure of wall-attached bubbles influenced the release of TDG from water. Therefore, an experiment was performed to simulate the growth of wall-attached bubbles at various water flow velocities, a quantitative relationship between the wall-attached bubble growth period and flow velocity was obtained. Another quantitative relationship, between the wall-attached bubble departure diameter and turbulent kinetic energy of flowing water, was also determined. The analysis results of the TDG release rate proved that the adsorption of TDG on solid walls was considerably affected by flow velocity. The analysis models the TDG release mechanism through complex experiments and provides a method to better identify sites for supersaturated TDG adsorption. This study serves as an important theoretical basis for revealing the mechanism by which solid surfaces promote the release process of supersaturated TDG in natural water.

**Key words:** flow velocity, growth period, supersaturation, total dissolved gas, wall adsorption, wall-attached bubble

### HIGHLIGHTS

- The growth rate and number density of wall-attached bubbles were mainly affected by TDG saturation.
- The flow velocity promoted the departure frequency of wall-attached bubbles.
- The solid wall area had a clear impact on TDG release rate.

### NOTATION

The following symbols are used in this paper:

$A$	projected bubble area ( $\text{mm}^2$ )
$a_w$	specific solid wall area of supersaturated water ( $\text{m}^{-1}$ )
$a_s$	specific surface area of supersaturated water ( $\text{m}^{-1}$ )
$C$	TDG concentration ( $\text{mg/L}$ )
$E_w$	wall adsorption flux of supersaturated TDG ( $\text{mg}\cdot\text{m}^{-2}\text{min}^{-1}$ )
$F_G$	release rate of supersaturated TDG ( $\text{mg}\cdot\text{L}^{-1}\text{min}^{-1}$ )
$F_s$	release rate of supersaturated TDG from air-water mass transfer ( $\text{mg}\cdot\text{L}^{-1}\text{min}^{-1}$ )
$F_w$	release rate of supersaturated TDG from wall adsorption ( $\text{mg}\cdot\text{L}^{-1}\text{min}^{-1}$ )
$F_{in}$	release rate of supersaturated TDG from inside water ( $\text{mg}\cdot\text{L}^{-1}\text{min}^{-1}$ )
$F_a$	buoyancy of wall-attached bubble (N)
$F_v$	shear force provided by turbulence (N)
$F_y$	viscous force provided by the experiment flume wall (N)
$G$	saturation of TDG (%)
$h$	water depth (m)
$k_{in}$	TDG internal release coefficient ( $\text{min}^{-1}$ )
$K_s$	mass transfer coefficient of air-water interface ( $\text{m}\cdot\text{min}^{-1}$ )
$N$	wall-attached bubble number density ( $\text{cell}/\text{cm}^2$ )
$t$	time (min)
$T_i$	surface turbulent kinetic energy ( $\text{m}^2/\text{s}^2$ )
$u_i$	time-averaged velocity (m/s)
$V_d$	departure bubble volume ( $\text{mm}^3$ )

This is an Open Access article distributed under the terms of the Creative Commons Attribution Licence (CC BY 4.0), which permits copying, adaptation and redistribution, provided the original work is properly cited (<http://creativecommons.org/licenses/by/4.0/>).

$X$	bubble retention time from formation to departure (min)
$\rho_B$	air density in wall-attached bubbles (mg/L)
$\rho_l$	water density (g/L)
$\tau$	shear stress caused by water flow near the experiment flume wall (N/m <sup>2</sup> )

## 1. INTRODUCTION

In the natural environment, dam discharge, waterfalls, sudden rise of water temperature and oxygen production by photosynthesis may lead to total dissolved gas (TDG) supersaturation in water. Due to the pressure difference between water and the atmosphere, supersaturated TDG in water is slowly released to the atmosphere (Li *et al.* 2009). Supersaturated TDG exist for a long time in water, which may cause fish suffering due to gas bubble disease or even death and have serious adverse effects on aquatic ecology (Weitkamp 2000). The release rates of TDG are directly related to the TDG levels and the pressure difference between water and the atmosphere (Lu *et al.* 2019). The partial pressure of gas within bubbles is usually different from the gas in the liquid phase, and supersaturated TDG dissolved in water form suspended bubbles. The exchange of TDG at the water-gas phase interface plays a key role in the TDG transport process. A bubble in TDG supersaturated water may be defined as a self-contained body of TDG that is separated from its surrounding medium by a recognizable interface (Clift *et al.* 1978). When gas transfer occurs at the bubble interface, the bubble grows, and the TDG concentration in water changes. Numerical models to predict the TDG distribution and release process based on bubble size and bubble number density have been developed (Politano *et al.* 2004), and mathematical models of the mass transfer of air from bubbles to water have been proposed (Takemura 1998). In fluid computational models for TDG release process prediction, the bubble size distribution in water and the gas volume fraction are the key parameters (Politano *et al.* 2017).

In practical engineering applications that involve the transportation of water, dissolved gas molecules collide and attach to solid surfaces, such as suspended solids and vegetation in the water. A previous study proved that this effect, which can be described as solid wall absorption, is an effective method for enhancing the TDG release process (Yuan *et al.* 2018). Based on experiments focusing on the adsorption effect of solid walls, a quantitative relationship between the adsorption coefficient and contact angle of solid surfaces was obtained (Yuan *et al.* 2020). The rate of the TDG release process depends on the bubble parameters such as diameter, which depends on the partial gas pressure within bubbles and the supersaturated TDG concentration in water and affects the surface area for mass transfer and bubble growth time (Ahmed & Semmens 2003). Grinin *et al.* (2009) considered that the factors affecting the bubble growth rate include temperature, pressure and dissolved gas concentration in gas-liquid mixtures. Li *et al.* (2016) improved the prediction equations for bubble escape diameter and frequency which have been proposed by Zuber (1963) and obtained relationships between surface tension, liquid density and equilibrium bubble diameter. However, the mechanism by which wall-attached bubbles promote the adsorption of supersaturated TDG on solid surfaces was not revealed in the above studies, and an understanding of wall-attached bubble adsorption and escape in flowing water is still lacking in the TDG concentration prediction study field.

In previous experiments, the dissipation coefficient was used to quantify the degassing process of TDG saturation. The characteristic parameters affecting the diameter and number density of wall-attached bubbles play a key role in supersaturation TDG adsorption on solid walls. Therefore, in this paper, an experiment was conducted to observe the adsorption and release of bubbles from solid surfaces, the effects of the solid wall area on the supersaturated TDG release process were studied, and the results are reported to provide an innovate theoretical basis for predicting the supersaturated TDG release coefficient.

## 2. EXPERIMENTAL STUDY OF THE GROWTH CHARACTERISTICS OF WALL-ATTACHED BUBBLES UNDER FLOWING WATER CONDITIONS

### 2.1. Materials and methods

The experiment was conducted in the State Key Laboratory of Hydraulics and Mountain River Development and Protection (Sichuan University, China). The experimental device was a Plexiglas flume (50 cm in width, 1500 cm in length, and 30 cm in height, with a slope of 0.045%), and a baffle was set at the lower part of the flume to maintain the water depth. The velocity and turbulent kinetic energy of flowing water were measured by an Acoustic Doppler Velocimetry (ADV) produced by Nortec Company. ADV can measure the distance from the probe to the bottom of the flume at a frequency of 10 Hz, the flow rate measurement range is 0–3 m/s, and the accuracy is 1 mm/s. The TDG saturation level in the water was measured by a total dissolved gas pressure (TGP) detector composed of Pentair Point Four TGP portable trackers (California, USA) with a TGP

measuring range of 0–200% and an accuracy of 2%. The experimental equipment used to observe wall-attached bubble growth characteristics under flowing water conditions is shown in Figure 1.

The bubble development and escape processes on the wall of the water flume was tracked and photographed by a digital camera. The photographic equipment consisted of a Canon 600D digital camera with 17–85 lenses (Taiwan), a polarizer, and a close-up lens for taking close-up pictures. The back of the experimental water flume was arranged against a black background to ensure clear images during the experiment, the light source was an LED lamp that provided a uniform distribution of light on the top of the water flume, and the camera was fixed in front of the water flume. The photographic equipment used in the experiment is shown in Figure 2. The experiment was performed under atmospheric pressure. Super-saturated TDG water was provided by the supersaturated TDG generation system developed by Sichuan University in China (Li *et al.* 2010), where the generated maximum supersaturated TDG level was 170%. The water temperature in the experimental flume was maintained at 20 °C throughout the experimental process.

Five TDG saturation conditions and five flow conditions were used in the experiment to study the influence of flow velocity and TDG saturation on the growth of wall-attached bubbles. A flow velocity of 0 cm/s was the control condition, and there was a total of 25 experimental cases, as shown in Table 1.

The velocity measuring points were distributed in the x-0-y plane, and the turbulent kinetic energy measuring points were distributed in the x-0-z plane. The layout of the measuring points and the schematic diagram of the measuring device are shown in Figure 3.

## 2.2. Measurement results for flow velocity and turbulent kinetic energy

Turbulent kinetic energy ( $T$ ) is a hydraulic factor describing the turbulence of the water flow. The formula used to calculate the turbulent kinetic energy at the sidewall of the experimental flume is as follows in Equation (1) (Tan *et al.* 2017):

$$T_i = \frac{1}{2}(u_{i,x}^2 + u_{i,y}^2 + u_{i,z}^2) \quad (1)$$

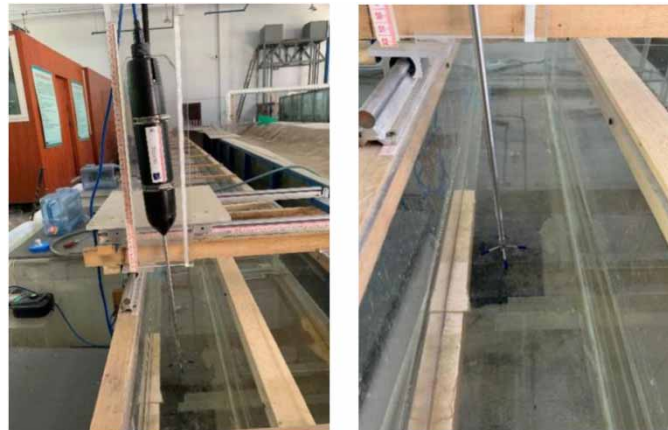


**Figure 1** | Experimental equipment used to study wall-attached bubbles growth characteristics under flowing water conditions.

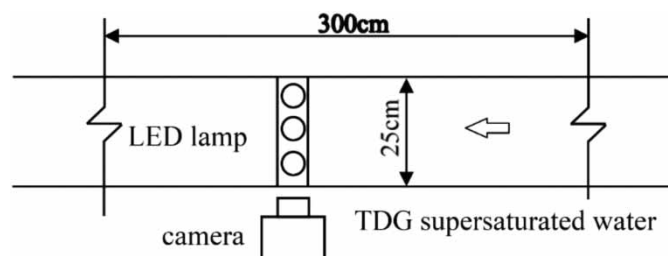


**Figure 2** | Diagram of the photographic equipment used in this experiment.

**Table 1** | Conditions of the experimental cases

Case number of TDG supersaturation	G (%)	Case number of flow velocity	Q (L·s <sup>-1</sup> )
1	120	a	0
2	130	b	4.43
3	140	c	6.98
4	150	d	10.27
5	160	e	14.34

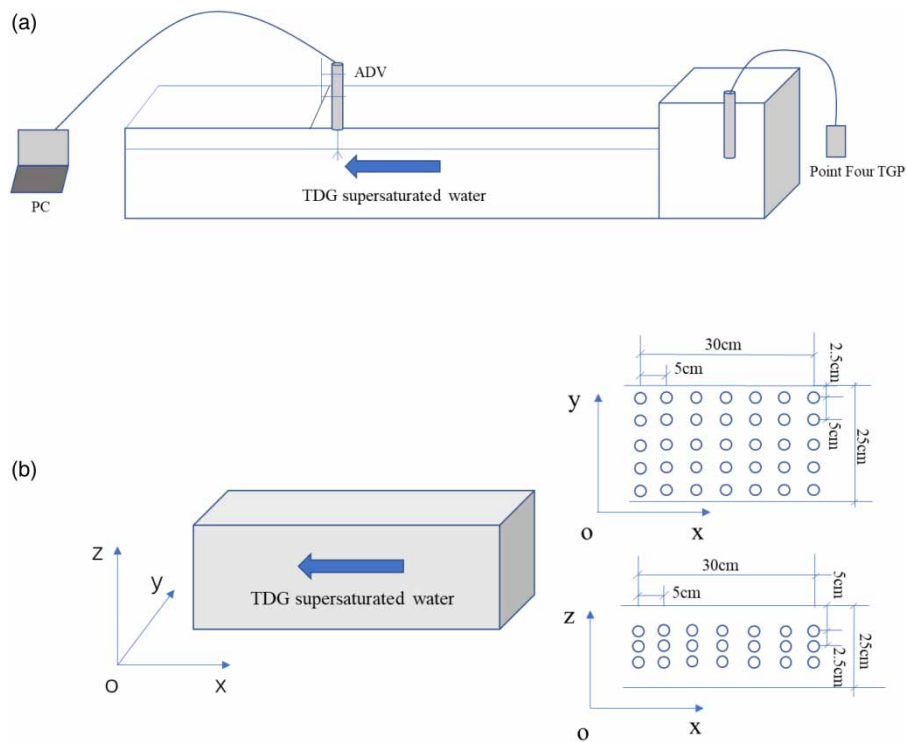


**Figure 3** | Diagram of the experimental velocity measuring equipment. (a) Diagram of the experimental velocity measuring method. (b) ADV measuring points in the flume.

where  $T_i$  and  $u'_i$  represent the turbulent kinetic energy ( $m^2/s^2$ ) and instantaneous velocity (m/s) at point  $i$  and satisfy the following relationship as shown in Equation (2):

$$u'_i = u_i - \bar{u}_i \tag{2}$$

where  $\bar{u}_i$  represents the time-averaged velocity (m/s) and  $u'_{i,x}$ ,  $u'_{i,y}$ , and  $u'_{i,z}$  are the pulsating velocities in three directions,  $x$ ,  $y$  and  $z$  ( $m \cdot s^{-1}$ ).

$\bar{T}$  represents the average turbulent kinetic energy at the sidewall of the flume according to Equation (3):

$$\bar{T} = \frac{1}{n} \sum_{i=1}^n T_i \tag{3}$$

The measurement results for the flow cases are shown in Table 2.

**Table 2** | The measurement results for the flow cases

Case no.	Water depth (cm)	Average velocity (cm·s <sup>-1</sup> )	Average turbulent kinetic energy (cm <sup>2</sup> ·s <sup>-2</sup> )
a	17	0	0
b	16.1	11	2.88
c	14.0	20	7.28
d	14.7	28	10.15
e	13.9	35	31.28

### 3. WALL ADSORPTION EFFECTS OF TDG BASED ON WALL-ATTACHED BUBBLES

#### 3.1. Analysis of the wall-attached bubble departure diameter

According to observations during the experiment, wall-attached bubbles depart from the wall when they grow to a certain diameter (Chen & Qiu 2015). Unlike wall-attached bubbles in static water that completely rely on buoyancy to depart from the wall, wall-attached bubbles in flowing water undergo shear stress generated by turbulence. Under flowing conditions, wall-attached bubbles leave the wall when the combined forces of shear and buoyancy become larger than the viscous force of the wall. Ignoring gravity, a stress analysis of a wall-attached bubble is shown in Figure 4. The relationship between the departure diameter of wall-attached bubbles and hydraulic conditions can be explained from the perspective of this experiment.

The force balance expression of wall-attached bubbles in flowing water is as follows in Equation (4):

$$\vec{F}_a + \vec{F}_v = \vec{F}_\gamma \quad (4)$$

where  $\vec{F}_a$  represents the buoyancy of the wall-attached bubble (N);  $\vec{F}_v$  represents the shear force provided by turbulence (N); and  $\vec{F}_\gamma$  represents the viscous force provided by the experimental flume wall (N).

The buoyancy of a wall-attached bubble  $F_a$  can be calculated by Equation (5):

$$F_a = 0.1\rho_B g V_d \quad (5)$$

where  $V_d$  represents the wall-attached bubble volume at the departure time, (mm<sup>3</sup>);  $\rho_B$  represents the gas density, (mg/L); and  $g$  represents the acceleration due to gravity, (m/s<sup>2</sup>).

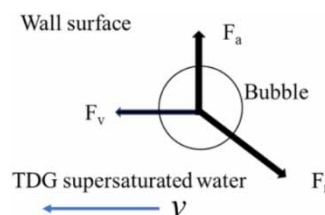
The shear force provided by flow turbulence  $F_v$  can be calculated by Equation (6):

$$F_v = \tau A'_d \quad (6)$$

where  $\tau$  represents the shear stress caused by water flow near the experimental flume wall (N/m<sup>2</sup>) and  $A'_d$  represents the projected area of the wall-attached bubble perpendicular to the flow direction at the departure time (mm<sup>2</sup>) (Lin *et al.* 2021).

The calculation method of  $\tau$  is as follows in Equation (7):

$$\tau = \rho_l \bar{T} \quad (7)$$

**Figure 4** | Stress analysis of a wall-attached bubble.

where  $\rho_1$  represents the water density ( $\text{kg/m}^3$ ) and  $\bar{T}$  represents the average turbulent kinetic energy at the sidewall of the flume ( $\text{m}^2/\text{s}^2$ ).

Fritz (1935) gave the relationship of the departure diameter of a wall-attached bubble and the contact angle  $\theta$  between bubbles and the wall, and the departure diameter of wall-attached bubbles in static water is related to the wall material. Taking the statistical value of the wall-attached bubble departure diameter in the state water case as the calibration condition, the departure diameter under different flow rates can be calculated according to Equations (4)–(7). The comparison of the calculated values and the experimental statistical values of the wall-attached bubble departure diameter is shown in Figure 5.

### 3.2. Analysis of the wall-attached bubbles number density

The experimental results showed that the number density of wall-attached bubbles was obviously different in water flows with different TDG saturations and velocities. The number density ( $\text{cell/cm}^2$ ) of wall-attached bubbles for each experimental case can be calculated by a program in MATLAB (Gonzalez & Woods 2007; Lin *et al.* 2021). The statistical results are shown in Figure 6.

Figure 6 shows that increasing the flow velocity decreases the wall-attached bubble number density. The quantitative relationship between the wall-attached bubble number density and the TDG supersaturation and flow velocity obtained by the nonlinear regression method is as follows in Equation (8):

$$N = 0.017e^{-0.031v}(G - 100\%)^{1.508} \tag{8}$$

where  $N$  represents the wall-attached bubble number density, ( $\text{cell}\cdot\text{cm}^{-2}$ );  $v$  represents the flow velocity, ( $\text{cm/s}$ ); and  $G$  represents the supersaturation of TDG (%).

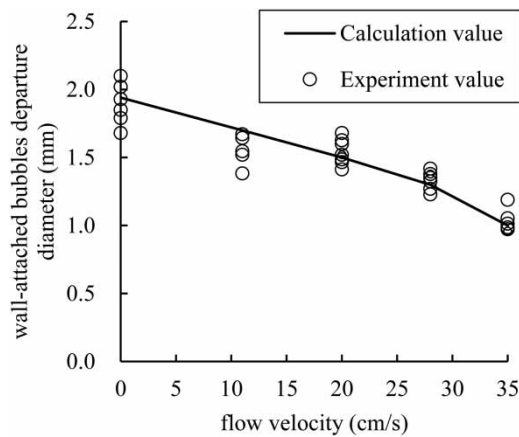


Figure 5 | Comparison of the calculated and experimental statistical values of the wall-attached bubble departure diameter.

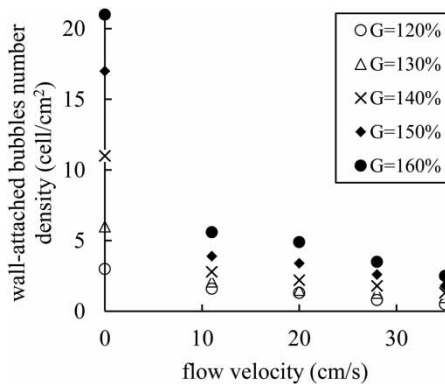


Figure 6 | Statistics of the wall-attached bubble number density.

The correlation coefficient is 0.986. The calculation result of Equation (8) and the statistical result for the wall-attached bubble number density are shown in Figure 7, and the error between the calculation and statistical values was within 25%.

### 3.3 Analysis of the wall-attached bubble growth time

The growth period of wall-attached bubbles can be described by the cumulative survival rate  $S(t)$ . At each time point, the ratio of bubbles grown on the wall to the total statistics number was recorded as the cumulative survival rate. The expression for  $S(t)$  is as follows in Equation (9):

$$S(t) = P(X > t) = 1 - P(X \leq t) = \int_t^{\infty} f(x) dx \quad (9)$$

where  $X$  represents the wall-attached bubble growth time (min);  $P(X > t)$  indicates the probability that the survival time of bubbles is greater than  $t$ ; and  $f(t)$  is called the distribution density function, which describes the distribution law of the bubble survival time.

The statistical results for the cumulative survival rate of wall-attached bubbles under experimental conditions are shown in Figure 8.

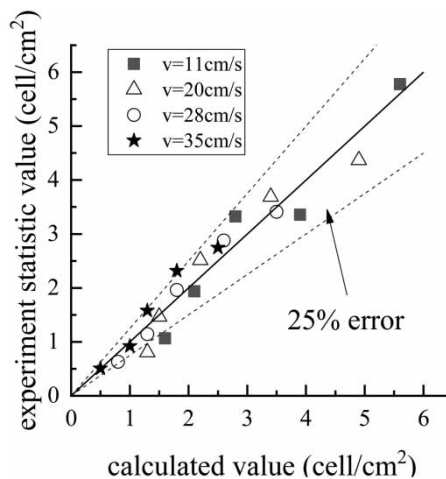
Figure 8 shows the ratio of the wall-attached bubbles staying on the wall at different times to the total number in the statistical time period. This figure shows that after the start of the evaluation of statistics, the wall-attached bubbles gradually escape. The statistical results show that the flow velocity can promote wall-attached bubble departure. According to the images of wall-attached bubbles recorded in the experiment, the average growth time of wall-attached bubbles under the experimental cases can be obtained. The statistical results of the average wall-attached bubble growth time are shown in Figure 9.

Figure 9 shows that increasing the flow velocity decreases the wall-attached bubble growth time. The quantitative relationship for wall-attached bubble growth time with TDG supersaturation and flow velocity was obtained by the nonlinear regression method as follows in Equation (10):

$$X = 141.3e^{-0.073v - 0.025(G - 100\%)} \quad (10)$$

where  $X$  represents the wall-attached bubble growth time (min);  $v$  represents the flow velocity (cm/s); and  $G$  represents the supersaturation of TDG (%).

The correlation coefficient is 0.964. The calculation result of Equation (10) and the statistical result of wall-attached bubble growth time are shown in Figure 10, the error between the calculation and statistical values was within 20%.



**Figure 7** | Comparison of the calculated and statistical values of the wall-attached bubble number density.

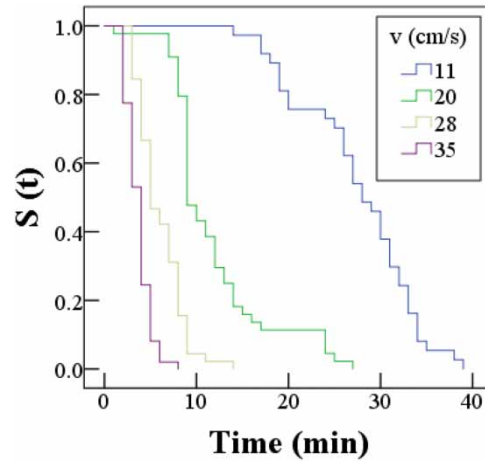


**Figure 8** | Statistical results for the cumulative survival rate of wall-attached bubbles.

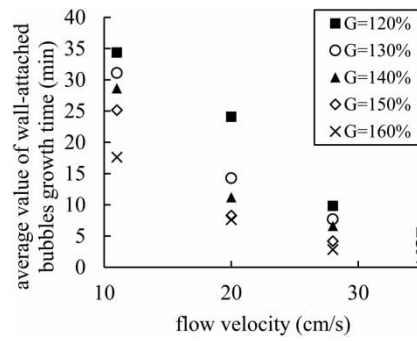


**Figure 9** | Statistical results of average wall-attached bubbles growth time.

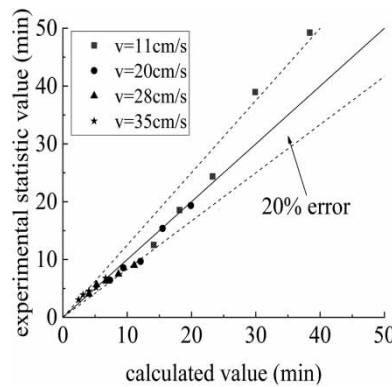


**Figure 10** | Comparison of the calculated and statistical values of the wall-attached bubble growth time.

### 3.4. Calculation of the wall adsorption flux for supersaturated TDG

The reliability of the proposed wall adsorption flux of TDG can be calculated as follows in Equation (11):

$$E_w = \frac{NV_d \rho_B}{X} \tag{11}$$



where  $E_w$  represents the wall adsorption flux of TDG ( $\text{mg}\cdot\text{m}^{-2}\text{h}^{-1}$ );  $N$  represents the wall-attached bubbles number density ( $\text{cell}/\text{cm}^2$ );  $V_d$  represents the wall-attached bubble volume at the departure time ( $\text{mm}^3$ );  $X$  represents the growth time of wall-attached bubbles (min); and  $\rho_B$  represents the gas density ( $\text{mg}/\text{L}$ ).

The wall adsorption flux of supersaturated TDG in flowing water was calculated as shown in Figure 11.

#### 4. CALCULATION OF THE TDG RELEASE RATE BASED ON WALL ADSORPTION

##### 4.1. Mathematical expression of the TDG release rate

Based on a previous study of the wall adsorption effect on the TDG release process, the calculation method for the supersaturated TDG coefficient based on wall-attached bubbles can be used to predict the TDG release process. The dissipation process of supersaturated TDG in water consists of three parts (Yuan *et al.* 2018). The amount of supersaturated TDG released in static water can be expressed according to Equation (12):

$$F_G = F_s + F_w + F_{in} \quad (12)$$

where  $F_G$  represents the total release rate of supersaturated TDG ( $\text{mg}\cdot\text{L}^{-1}\text{min}^{-1}$ ) and  $F_s$ ,  $F_w$ , and  $F_{in}$  represent the release rates of supersaturated TDG from air-water transfer, wall absorption, and internal release, respectively ( $\text{mg}\cdot\text{L}^{-1}\text{min}^{-1}$ ). Furthermore, Equation (13) shows  $F_G$ :

$$F_G = \frac{\Delta C}{\Delta t} \quad (13)$$

where  $\Delta C$  represents the supersaturated TDG variation value ( $\text{mg}\cdot\text{L}^{-1}$ ) and  $\Delta t$  represents the TDG release time (min).

$F_s$  can be calculated by Equation (14):

$$F_s = K_s a_s (C - C_{eq}) \quad (14)$$

where  $K_s$  represents the mass transfer coefficient of the air-water interface ( $\text{m}/\text{min}$ ),  $a_s$  represents the specific surface area of supersaturated water ( $\text{m}^{-1}$ ),  $C$  represents the concentration of supersaturated TDG ( $\text{mg}/\text{L}$ ), and  $C_{eq}$  represents the equilibrium concentration of supersaturated TDG ( $\text{mg}/\text{L}$ ).

The quantitative relationship between the mass transfer coefficient of the air-water interface and the surface turbulent kinetic energy was proposed by Li *et al.* (2000), as shown in Equation (15):

$$K_s = 0.085T_s^{1/2} + 0.0014 \quad (15)$$

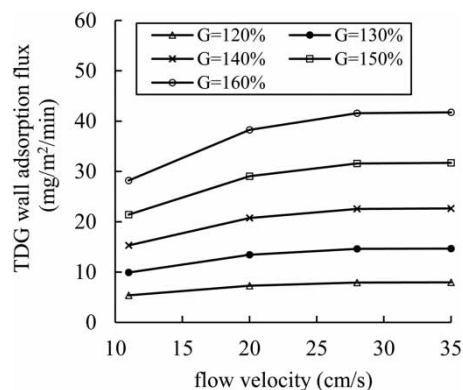


Figure 11 | Calculation values of the TDG wall adsorption flux for the experimental cases.

where  $T_s$  represents the surface turbulent kinetic energy ( $\text{m}^2/\text{s}^2$ ) and  $F_{\text{in}}$  can be calculated by Equation (16):

$$F_{\text{in}} = k_{\text{in}}(C - C_{\text{eq}}) \quad (16)$$

where  $k_{\text{in}}$  represents the TDG internal release coefficient ( $\text{min}^{-1}$ ).

The relationship between the TDG internal release coefficient and the water depth and flow pattern were obtained as follows in Equation (17) proposed by Huang (2017):

$$k_{\text{in}} = 0.0014F_r^{-0.22}h^{0.0053}e^{0.020a_w} \quad (17)$$

where  $F_r$  represents the Froude number;  $h$  represents the water depth (m); and  $a_w$  represents the specific surface area of the solid wall in water ( $\text{m}^{-1}$ ).

The reliability of the proposed wall adsorption flux was calculated as follows in Equation (18):

$$F_w = E_w a_w \quad (18)$$

where  $E_w$  represents the wall adsorption flux of supersaturated TDG ( $\text{mg}\cdot\text{m}^{-2}\text{min}^{-1}$ ) and  $a_w$  represents the specific surface area of the solid wall in water ( $\text{m}^{-1}$ ).

#### 4.2. Analysis of the wall adsorption effect on the TDG release rate

The data used to validate the supersaturated TDG release coefficient model was adopted from the measurements conducted by Huang (2017), who studied the influence of solid wall area and flow velocity on the TDG release coefficient. Huang (2017) designed a physical experiment to study the effects of flow characteristics and vegetation densities and assess the ability of vegetation to promote the dissipation of supersaturated TDG. During the experimental procedure, the flow velocity was constant, and the flow in the flume was steady. Vertical Plexiglas columns were used instead of rigid emergent plants. There were five groups of solid wall areas and five groups of flow velocities, resulting in a total of 25 experimental cases, as shown in Table 3.

The promotion effect of wall adsorption on the TDG release rate in flowing water is multifaceted. To clarify the proportion of wall adsorption in the TDG release rate under different flow velocity and vegetation density cases, a variable representing the promotion effect of wall adsorption on the TDG release rate is introduced  $\varepsilon$  (%). The expression for  $\varepsilon$  is as follows in Equation (19):

$$\varepsilon = \frac{F_{w,a}}{F_{G,a} - F_{G,a=0}} \times 100\% \quad (19)$$

where  $\varepsilon$  represents the effect of wall adsorption on the TDG release rate (%);  $F_{G,a}$  and  $F_{G,a=0}$  represent the release rates of supersaturated TDG using a solid wall with specific surface area  $a$  and  $a = 0$ , respectively ( $\text{mg}\cdot\text{L}^{-1}\text{min}^{-1}$ ); and  $F_{w,a}$  represents the release rate of supersaturated TDG from wall adsorption in the case of solid wall specific surface area  $a$  ( $\text{mg}\cdot\text{L}^{-1}\text{min}^{-1}$ ).

The calculation results of the  $\varepsilon$  value in the experimental cases are shown in Figure 12.

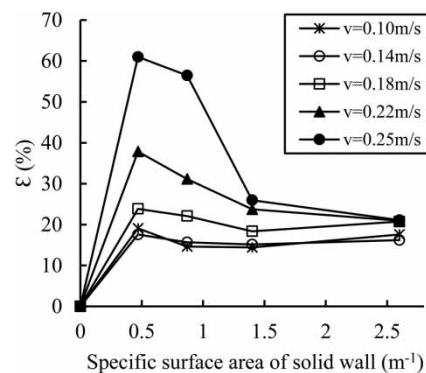
Figure 12 shows that under the conditions in which the specific surface area of the solid wall ranges are between 0.5 and  $1\text{ m}^{-1}$ , and the flow velocity is less than 0.14 m/s, the  $\varepsilon$  value ranges from 20 to 25%. When the flow velocity exceeds 0.25 m/s, the  $\varepsilon$  value reaches more than 60%. When the specific surface area of the solid wall is higher than  $1.5\text{ m}^{-1}$ , the  $\varepsilon$  value approaches 20%.

## 5. CONCLUSIONS

A quantitative relationship between the wall-attached bubble growth period and the flow velocity was obtained in this study. The analysis of the experimental results shows that the growth rate and number density of wall-attached bubbles were mainly affected by TDG saturation, and the quantitative relationship between the wall-attached bubble departure diameter and turbulent kinetic energy of flowing water shows that the flow velocity promoted the departure frequency of the wall-attached bubbles. The analysis result of the wall adsorption effects shows that the solid wall area had a clear impact on TDG release

**Table 3** | Conditions for the experimental cases (Huang 2017)

Case No.	Average flow velocity ( $\text{m}\cdot\text{s}^{-1}$ )	Specific surface area of the solid wall ( $\text{m}^{-1}$ )	TDG supersaturation (%)	
			Starting point	Ending point
1	0.1	0	144.5	137.2
2	0.1	0.47	144.2	135.2
3	0.1	0.87	144.9	133.5
4	0.1	1.4	145.3	131.3
5	0.1	2.6	145.7	128.2
6	0.14	0	144.4	138.9
7	0.14	0.47	144.6	137.8
8	0.14	0.87	147.4	139.2
9	0.14	1.4	145.9	135.9
10	0.14	2.6	147.5	134.2
11	0.18	0	145.6	140.2
12	0.18	0.47	144.5	138.3
13	0.18	0.87	148.5	141.5
14	0.18	1.4	147.5	139.0
15	0.18	2.6	148.5	138.0
16	0.22	0	147.1	142.0
17	0.22	0.47	146.6	141.1
18	0.22	0.87	148.6	142.6
19	0.22	1.4	147.8	140.8
20	0.22	2.6	149.3	140.2
21	0.25	0	148.1	143.9
22	0.25	0.47	147.9	143.5
23	0.25	0.87	149.0	144.4
24	0.25	1.4	148.6	143.0
25	0.25	2.6	149.7	142.3

**Figure 12** | Calculation results for  $\epsilon$ .

rate, the optimum value of the specific surface area was approximately between  $0.5$  and  $1 \text{ m}^{-1}$ . When the specific surface area exceeded  $1.5 \text{ m}^{-1}$ , the promotion effect on the TDG release rate came mostly from the internal release and the air-water mass transfer of TDG, which resulted from increased turbulence in flowing water by a solid wall.

However, in complex natural rivers, water flow is affected by topographical distributions and solid media vary greatly. Therefore, the analysis method of TDG release rate effects can be extended to take into account solid wall material and surface roughness. The proposed analysis method examines the TDG release mechanism through complex experiments and provides an important method to better identify supersaturated TDG adsorption sites.

## ACKNOWLEDGEMENTS

This work was supported by the National Natural Science Foundation of China (Grant No. 51879173) and the Key Program of the National Natural Science Foundation of China (Grant No. 52039006).

## DATA AVAILABILITY STATEMENT

All relevant data are included in the paper or its Supplementary Information.

## REFERENCES

- Ahmed, T. & Semmens, M. J. 2003 Gas transfer from small spherical bubbles in natural and industrial systems. *Journal of Environmental Systems* **29** (2), 101–123.
- Chen, X. D. & Qiu, H. H. 2015 Bubble dynamics and heat transfer on a wettability patterned surface. *International Journal of Heat and Mass Transfer* **88**, 544–551.
- Clift, R., Grace, J. R. & Weber, M. E. 1978 *Bubbles, Drops, and Particles*. Academic Press, Guildford.
- Fritz, M. F. 1935 The effect of diet on intelligence and learning. *Psychological Bulletin* **32** (5), 355–363.
- Fumio Takemura, A. 1998 Gas dissolution process of spherical rising gas bubbles. *Chemical Engineering Science* **53** (15), 2691–2699.
- Gonzalez, R. C. & Woods, R. E. 2007 *Digital Image Processing*, 3rd edn. Prentice-Hall, Inc, New Jersey.
- Grinin, A. P., Kuni, F. M. & Gor, G. Y. 2009 The rate of nonsteady gas bubble growth in liquid supersaturated with gas. *Journal of Molecular Liquids* **148** (1), 32–34.
- Huang, Y. H. 2017 *Impact of Vegetation on the Dissipation Process of Supersaturated Total Dissolved Gas*. Master's thesis. Sichuan University. (In Chinese).
- Li, R., Zhao, W. Q., Li, J. & Li, K. F. 2000 Experimental study on interfacial mass transfer coefficient of turbulent water. *Journal of Hydraulic Engineering* **31** (002), 60–65. (In Chinese).
- Li, R., Li, J., Li, K. F., Deng, Y. & Feng, J. J. 2009 Prediction for supersaturated total dissolved gas in high-dam hydropower projects. *Science in China* (12), 3661–3667.
- Li, R., Huang, X., Li, K. F., Yi, W. M. & Li, J. 2010 Device for Generation of Total Dissolved Gas Supersaturation in Water Body and Research on Influence of Total Dissolved Gas Supersaturation on Fish. CN 201479739U. (In Chinese).
- Li, Y. X., Zhang, K., Lu, M. C. & Duan, C. H. 2016 Single bubble dynamics on superheated superhydrophobic surfaces. *International Journal of Heat and Mass Transfer* **99**, 521–531.
- Lin, L., Li, R., Feng, J. J., Huang, Y. H., Yong, X. D., Ou, Y. M. & Yuan, Y. Q. 2021 Microanalysis of supersaturated gas release based on wall-attached bubbles. *Water Science and Engineering* **14** (1), 80–86.
- Lu, J. Y., Li, R., Ma, Q., Feng, J. J., Xu, W., Zhang, F. & Tian, Z. 2019 Model for total dissolved gas supersaturation from plunging jets in high dams. *Journal of Hydraulic Engineering* **145** (1), 04018082.1–04018082.10.
- Politano, M., Castro, A. & Hadjerioua, B. 2017 Modeling total dissolved gas for optimal operation of multireservoir systems. *Journal of Hydraulic Engineering* **143** (6), 04017007.
- Politano, M., Carrica, P., Turan, C. & Weber, L. 2004 Prediction of the total dissolved gas downstream of spillways using a two-phase flow model. In *World Water & Environmental Resources Congress*.
- Tan, J. J., Gao, Z. & Dai, H. C. 2017 The correlation analysis between hydraulic characteristics of vertical slot fishway and fish movement characteristics. *Journal of Hydraulic Engineering* **048** (008), 924–932, 944. (In Chinese).
- Weitkamp, D. E. 2000 *Total Dissolved Gas Supersaturation in the Natural River Environment*. PUD, Chelan county.
- Yuan, Y. Q., Feng, J. J., Li, R., Huang, Y. H., Huang, J. P. & Wang, Z. H. 2018 Modelling the promotion effect of vegetation on the dissipation of supersaturated total dissolved gas. *Ecological Modelling* **386**, 89–97.
- Yuan, Y. Q., Huang, J. P., Wang, Z. H., Gu, Y., Li, R., Li, K. F. & Feng, J. J. 2020 Experimental investigations on the dissipation process of supersaturated total dissolved gas: focus on the adsorption effect of solid walls. *Water Research* **183** (2020), 116087.
- Zuber, N. 1963 Nucleate boiling: the region of isolated bubbles and the similarity with natural convection. *International Journal of Heat & Mass Transfer* **6** (1), 53–60.

First received 4 January 2022; accepted in revised form 1 April 2022. Available online 13 April 2022